

Theoretical Models of Interacting Winds in Massive Binaries

Julian Pittard¹

¹ School of Physics and Astrophysics, University of Leeds, United Kingdom

Abstract: Massive binary systems are excellent laboratories for studying stellar winds. The powerful collision of the winds unleashes a broad spectrum of emission revealing the interesting physics of high Mach number shocks, including the acceleration of a small proportion of particles to relativistic energies. The wind-wind collision is also useful for probing the underlying wind and stellar parameters. This paper reviews our current understanding of the dynamics of such systems and models of (predominantly) the non-thermal emission, finishing with a brief note on possible future advances.

1 The Dynamics of Colliding Wind Binaries

1.1 Instabilities

In binary systems, the winds collide between the stars (or the stronger wind overwhelms its companion's wind, and crashes directly onto its surface). Therefore, it should come as no surprise that colliding wind binaries (CWBs) are an extremely diverse class of systems, with a very wide range of properties. To zeroth order, the nature of a particular CWB depends on the orbit of its stars. In short period systems, where the two stars are very close together, the wind-wind collision is likely to be highly radiative. The shock-heated gas therefore cools very rapidly, and a geometrically thin and dense region of gas forms which is prone to severe, and perhaps disabling, non-linear thin-shell instabilities (NTSI, Vishniac 1994)¹. On the other hand, if the orbital period is long, the shocked gas may behave largely adiabatically, flowing out of the system while still hot. In this case the wind-wind collision region (WCR) stays thick and “puffed-up”, and is far less affected by instabilities. Kelvin-Helmholtz instabilities, due to a velocity shear at the contact discontinuity between the winds, may occur in this case. Where one wind is radiative and the other largely adiabatic, a thin dense layer of cooled gas abuts a thicker, hotter, but more rarefied layer which acts like a “cushion” to damp out thin shell instabilities occurring in the dense layer (Vishniac 1983). These differences were illustrated by Stevens et al. (1992), and are reproduced in Fig. 1.

The transition between radiative and adiabatic post-shock regions is conveniently estimated using the value of $\chi \equiv t_{\text{cool}}/t_{\text{dyn}} \approx v_8^4 D_{12}/\dot{M}_{-7}$, where t_{cool} is the cooling time of the gas, t_{dyn} is a dynamical flowtime which is rather loosely defined but can be taken as either the time for shocked

¹This is the conventional wisdom, but in fact it is not clear exactly what occurs between the stars - e.g. even whether two “winds” are produced - in such an extreme and hostile environment.

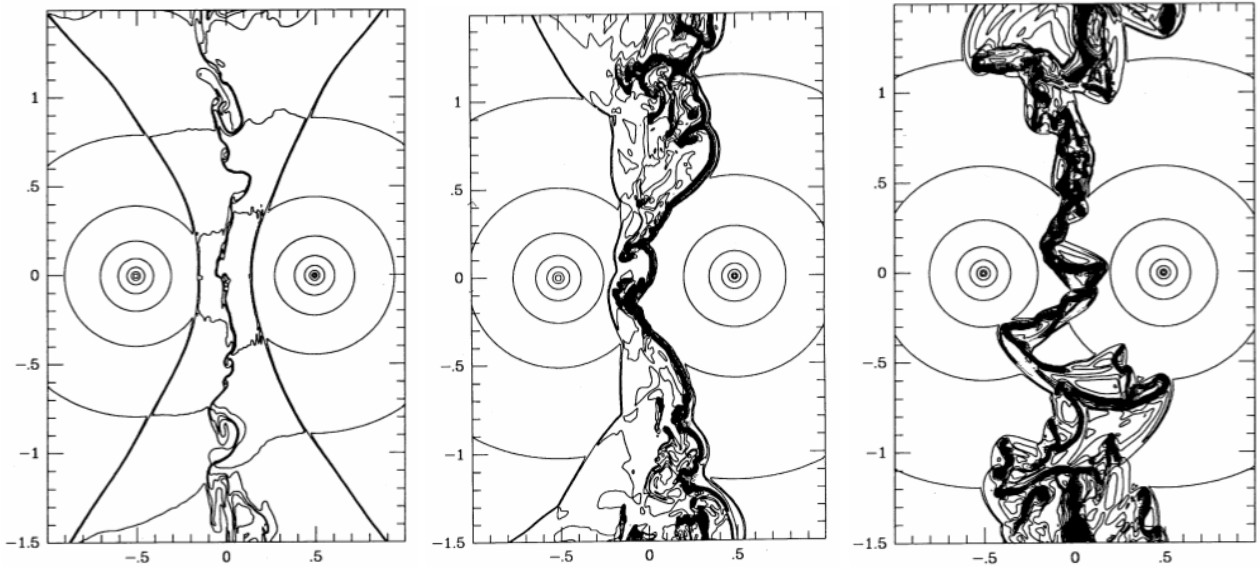


Figure 1: Instabilities in the WCR of CWBs. Left: When both sides of the contact discontinuity are largely adiabatic, the WCR is very smooth. Center: When one side is radiative thin shell instabilities occur, but are somewhat limited by the “cushioning” of the hot gas (Vishniac 1983). Right: When both sides are radiative, the much stronger and highly non-linear thin shell instability occurs (Vishniac 1994). Adapted from Stevens et al. (1992).

gas at the apex of the WCR to flow a distance D_{sep} downstream, or for the shocked gas from the weaker wind to flow a distance r_{OB} downstream (see Stevens et al. (1992) for these definitions). In the above, v_8 is the wind speed normalized to 1000 km s^{-1} , D_{12} is the stellar separation normalized to 10^{12} cm , and \dot{M}_{-7} is the mass-loss rate normalized to $10^{-7} M_{\odot} \text{ yr}^{-1}$. Note that this formalism for χ depends on specific assumptions about the post-shock temperature and the morphology of the cooling curve at this point (see Pittard & Stevens 2002). By specifying appropriate values for \dot{M}_{-7} , etc., it is possible to determine a separate value of χ for each shocked wind. Values of χ in several key systems are listed in Pittard et al. (2005a).

1.2 Radiative Driving Effects

Early hydrodynamical models of the WCR were 2D, axisymmetric, and ignored orbital motion and radiative driving. The self-consistent transition between adiabatic and radiative behaviour was a key improvement in Stevens et al. (1992) compared to earlier work (e.g. Luo et al. 1990). Up until this point, all works modelled the winds as colliding at their terminal speed (or some fraction of this), and conveniently ignored the acceleration of the winds. This assumption is valid in long period systems, where the winds have room to accelerate before colliding, but is clearly not so when the stars are relatively close together. The effect of a nearby opposing radiation field was first explored by Stevens & Pollock (1994), where an effect termed “radiative inhibition” was noted. In this scenario the acceleration between the stars of one wind is inhibited by the radiation field of the other star, thus reducing the speed of the wind. A complementary effect, termed “radiative braking”, was studied by Gayley et al. (1997). This effect comes into play in systems where the stronger wind closely approaches the more luminous star. This condition is met in many Wolf-Rayet (WR) + O-star binaries. The stronger radiation field may then efficiently couple to the more powerful wind, causing a sudden deceleration or braking. The effect is highly non-linear, and the braking can be so severe that the stronger wind can be prevented from colliding with the surface of the more luminous star even in

cases where a normal ram-pressure balance between the winds would not be possible.

1.3 Orbital Effects

The first 3D models of CWBs published in a refereed journal were presented by Lemaster et al. (2007), with a focus on the effect of orbital motion. This causes the WCR to twist as the hot gas flows out of the system, creating an effect which resembles an Archimedian spiral. However, this investigation was highly simplified in that it lacked several key processes which are important in the short-period systems where the effects of orbital motion are greatest. The most notable omissions were the lack of any treatment for the acceleration of the winds and the cooling of the shocked gas. Shortly afterwards, 3D smoothed-particle-hydrodynamics (SPH) simulations of the WCR in the massive binary system η Carinae were presented (Okazaki et al. 2008). Though these models were isothermal, and did not solve for the temperature structure behind the shock, they provided much insight into the dynamics of the WCR in this highly eccentric ($e \approx 0.9$) system.

At about the same time, a “dynamic” model was presented by Parkin & Pittard (2008). This model did not solve the hydrodynamic equations, but instead mapped the apex of the WCR (given by the equations in Stevens et al. 1992) into a 3D space. The apex was provided with a time-dependent skew which aimed to reflect the ratio of the wind to orbital speeds, and the gas was assumed to behave ballistically further downstream. Though the resulting dynamics are only representative of the true situation, a comparison against results from a full hydrodynamical calculation revealed that this approach does a more than adequate job in many situations. Its great power, of course, is its speed, with a full 3D orbital calculation taking only seconds to run. It is then a simple matter to map appropriate emissivities onto the contact surface of the winds and perform ray-tracing through the volume. This method was also applied to a study of η Carinae, and revealed that contrary to the conclusion of Okazaki et al. (2008), the observed X-ray minimum could not be explained by an increase in absorption as the denser wind of the LBV primary moves in front of the apex of the WCR (Parkin et al. 2009). In fact, it now seems that the action of instabilities like those shown in Fig. 1 may play a key role in explaining the minimum (Parkin et al. 2011, submitted).

The first 3D simulations of CWBs to include orbital motion, the radiative driving of the winds and cooling of the shocked gas were presented by Pittard (2009). Focusing on O+O-star systems, this work showed that in a short period (3 d) system, the low speed of the winds between the stars prior to their collision (730 km s^{-1}) led to rapid cooling ($\chi \ll 1$) and the generation of a cold dense sheet of compressed gas. This sheet is susceptible to instabilities, and dense clumps break-off which are surrounded by bowshocks and hot shocked gas. However, the instabilities develop slightly differently from the equivalent case without orbital motion. This is because the high inertia of the dense shell causes it to move to the trailing edge of the WCR as the stars move around on their orbits. This curvature means that downstream the leading edge becomes quite rarefied and remains hot, such that this gas acts as a cushion against run-away development of the NTSI. It will be interesting to see if the NTSI occurs in systems which are even more radiative.

A system with the same stars as the previous case but where the orbital period was increased to 10 d displays totally different behaviour. This is due to the increased distance between the stars which allows the winds to accelerate to higher speeds before they collide (1630 km s^{-1}), and for the shocked gas to be hot and rarefied enough for it to remain largely adiabatic ($\chi \sim 40$) as it flows out of the system. The WCR is now very smooth, with small Kelvin-Helmoltz instabilities along the contact surface the only disturbance. The twisting of the WCR due to orbital motion is also less severe.

The most interesting dynamics occurred in an eccentric system ($e = 0.36$) where the periastron and apastron separations were chosen to match the orbital separations in the two previous simulations. The WCR displays a strong hysteresis through the orbit (see Fig. 2), with marked differences

in its properties when the stars are at identical stellar separations but approaching or receding from periastron. For instance, the gas in the WCR remains hot until near phase 0.9, after which it collapses into a thin dense sheet which is torn apart by instabilities. However, it is not until after apastron that the cold clumps are cleared away from the stars. This is again due to their high inertia relative to the rarefied gas which flows past them. During the transition between a radiative and largely adiabatic WCR (as χ goes from $\ll 1$ to ~ 40), the radiative overstability (e.g. Strickland & Blondin 1995; Pittard et al. 2005b) is seen. More recently, the dynamics of WR+O-star binaries have been investigated by Parkin et al. (2011, submitted - see also this volume).

Studies of how wind clumping affects the WCR have been presented by Walder (1998), who showed that dense clumps can tip an otherwise marginally adiabatic WCR into a radiative regime. Pittard (2007) examined the effect of clumps on an adiabatic WCR. If the clumps are not too dense or large (so that they do not punch through the WCR), they can be rapidly destroyed by the vorticity created during their passage through the shocks bounding the WCR. Although the WCR becomes highly turbulent as a result, the overall effect is to smooth out the flow. Thus determinations of the stellar mass-loss rates using the emission from a WCR may be relatively insensitive to clumping, and thus offer a useful alternative to other methods where this is not the case. The strong turbulence occurring within the WCR also has implications for particle acceleration and the mixing of the winds.

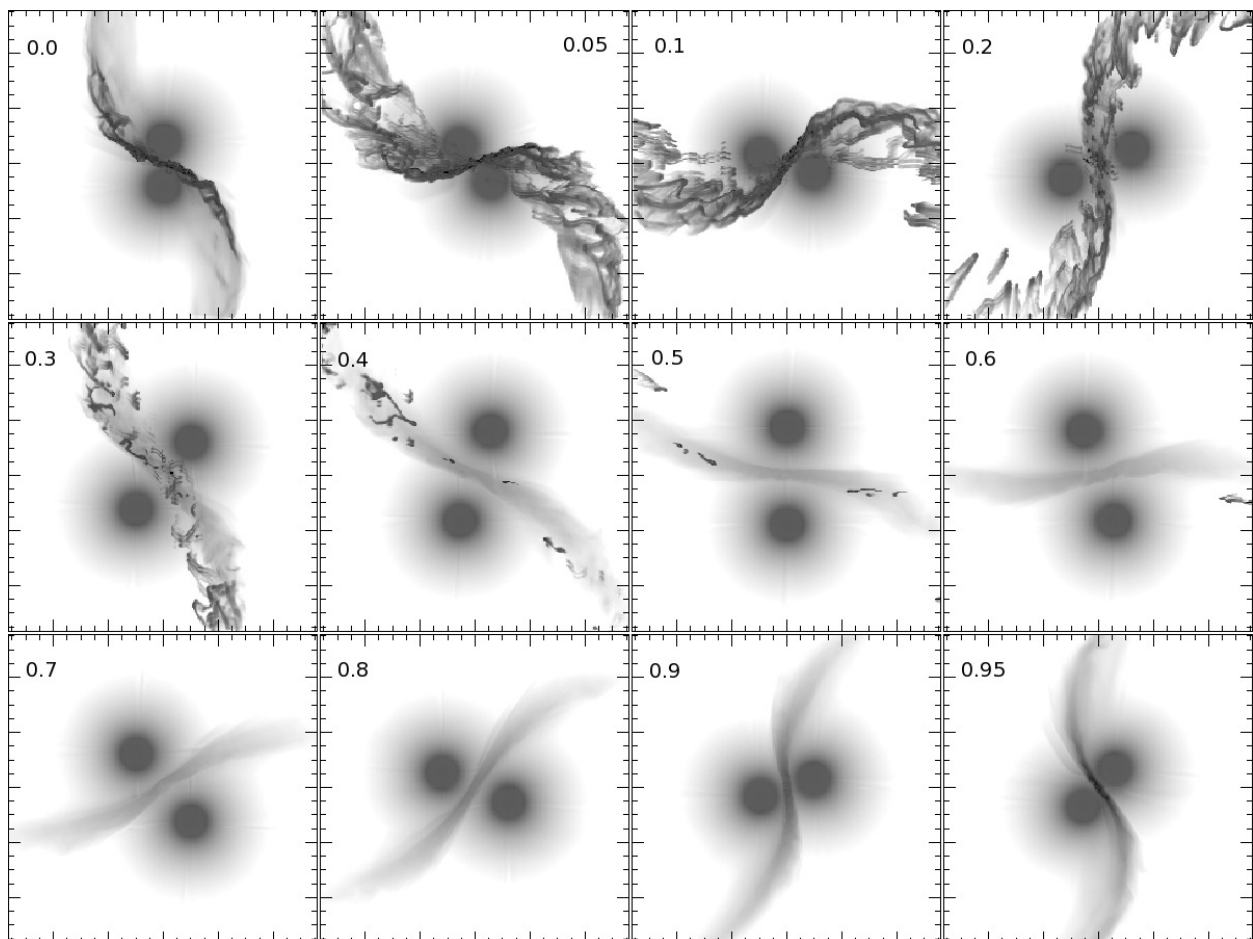


Figure 2: Intensity images at 1000 GHz for an observer viewing an eccentric ($e = 0.36$) O+O-star system with an orbital period of 6.1 d (see Pittard (2009) for details of the hydrodynamical model).

2 Modelling CWB Phenomena

Models of the WCR in CWBs can help to determine:

1. The mass-loss rate and wind speed (for instance from the X-ray emission - see e.g. Stevens et al. 1996 and Pittard & Corcoran 2002). The thermal radio emission from close binaries may also be used to determine the mass-loss rates.
2. The wind momentum ratio and flow speed in the WCR (the latter as measured from line-profiles).
3. The ionization timescale of the shock-heated gas (from X-ray line profiles - see Pollock et al. 2005).
4. The particle acceleration efficiency and the magnetic field strength (by comparing against the non-thermal emission - see Pittard et al. 2006).

To model the emission from the WCR with hydrodynamic codes, one must resolve the cooling length behind the shock. This is a difficult task when the cooling is very rapid. To overcome this problem, Antokhin et al. (2004) developed a model which decoupled the small-scale post-shock cooling from the large-scale structure of the collision region. This was subsequently employed to interpret data on HD 159176 (De Becker et al. 2004). However, a central assumption is that the global structure is stable, but as we have seen in Fig. 1, when the cooling is rapid the action of instabilities becomes dynamically important.

One of the most important models in the last decade or so is the Lührs model (and its subsequent improvements) for fitting the profile variability of IR, optical and UV lines (Lührs 1997). In this model it is assumed that the excess emission on top of flat-topped emission lines is from material flowing along the shock cone (i.e. the WCR). This excess can be parameterized by two quantities: the full width of the excess emission (at some suitable height), and the mean radial velocity of the excess. Lührs (1997) derived simple relationships between these quantities and values for the orbital inclination, the half-opening angle of the WCR, and the skew of the WCR due to orbital effects. Fitting the model to the observed phase-dependent profiles yields for these parameters. However, its application to systems with highly eccentric orbits should be made with care, because significant orbit induced curvature of the WCR can be misinterpreted as a large opening angle, and therefore the wind momentum ratio can be wrongly inferred. In such cases, a model which accounts for curvature of the WCR (and not just its skew angle) is needed. Models of X-ray line profile formation in the WCR have been presented by Henley et al. (2003, 2005, 2008).

2.1 Models of the Non-thermal Radio Emission

Direct evidence for non-thermal emission from a CWB was presented by Williams et al. (1997). UKIRT shift-and-add IR images overlaid on radio images of WR 147 revealed that when the southern (WR) star was aligned with the southern (thermal) radio source, the northern (non-thermal) radio source was found to lie just south of the northern (O) star, in a position consistent with the point of ram-pressure balance between the winds. Further support for this picture has been provided by direct imaging of the WCR in WR 146 and WR 140 (Dougherty et al. 2000, 2005). While there are many possible mechanisms for accelerating particles, it is normally assumed that diffusive shock acceleration (DSA) is the dominant process. A detailed discussion of other possibilities can be found in Pittard & Dougherty (2006).

The non-thermal radio emission from the WCR escapes easily from WR 146 and WR 147, which are both very wide and likely have orbits with periods of thousands of years, but has a much harder

job escaping from WR 140, due to its much tighter, highly eccentric, orbit of 7.94 yr period where the stellar separation varies between $\approx 1.5 - 28$ AU. The radio emission shows dramatic, phase-repeatable, modulations, at least part of which can be expected to be caused by variable circumstellar extinction to the source of the non-thermal emission as the O star orbits in and out of the radio photosphere in the dense WR wind. More recently, this system has been imaged with the VLBA, yielding a full orbit definition, including, most importantly, the inclination of the system (Dougherty et al. 2005). A pro-Am campaign to monitor WR 140 through periastron passage has further tightened the orbital elements (Fahed et al. 2011). However, while these studies have helped to provide some of the best modelling constraints of any system, relatively little is known about the wind of the O-star, and the wind momentum ratio remains ill-constrained.

Early models of the non-thermal radio emission from CWBs were very simple. It was usually assumed that the observed flux (S_ν^{obs}) was a combination of the free-free flux from the spherically symmetric winds (S_ν^{ff}), plus the flux from a point-like non-thermal source located at the stagnation point of the winds (S_ν^{nt}). In this model the non-thermal emission is then attenuated by free-free absorption (optical depth τ_ν^{ff}) through the surrounding winds:

$$S_\nu^{\text{obs}} = S_\nu^{\text{ff}} + S_\nu^{\text{nt}} e^{-\tau_\nu^{\text{ff}}}. \quad (1)$$

While this approach allows simple solutions to the radiative transfer equation (e.g. Williams et al. 1990; Chapman et al. 1999), such models fail to reproduce the spectral variation of the emission with orbital phase. Clearly their level of realism needed to be improved. Williams et al. (1990) therefore proposed that in future models of WR 140 the low-opacity “hole” in the dense WR wind created by the O-star’s wind should be accounted for. However, White & Becker (1995) pointed out that in WR 140, even the O-star’s wind has significant opacity. Together, these works demonstrated the need for more realistic models which account for the spatial extent of the emission and absorption from the circumbinary envelope and the WCR. More realistic models should also account for the effects of various cooling mechanisms (e.g. inverse Compton, adiabatic, etc.) on the non-thermal electron distribution, and also additional absorption mechanisms (e.g. the Razin effect).

Major improvements in the modelling of the radio emission were made by Dougherty et al. (2003), where key assumptions in previous models, such as a point-like source of non-thermal emission, and a spherically symmetric, single temperature, surrounding envelope, were removed. Models of the thermal and non-thermal radio emission were instead based on 2D, axisymmetric, hydrodynamical simulations, allowing a more accurate description of the density and temperature structure of the system. This meant that sight-lines to the observer can pass through regions of both high and low opacity. The assumption of a point-source of non-thermal emission was also removed, by treating the emission in a phenomenological way. Accelerated electrons were assumed to be present within the WCR, with an energy density ($U_{\text{rel,e}}$) proportional to the local thermal energy density (U_{th}) i.e. $U_{\text{rel,e}} = \zeta_{\text{rel,e}} U_{\text{th}}$. The magnetic field energy density was specified in a similar manner: $U_{\text{B}} = \zeta_{\text{B}} U_{\text{th}}$. The non-thermal electrons were further assumed to have a power-law distribution, $N(\gamma)d\gamma = C\gamma^{-p}d\gamma$, where γ is the Lorentz factor, C is proportional to $\zeta_{\text{rel,e}}$, and it was assumed that $p = 2$ (suitable for test particle DSA, with strong shocks and an adiabatic index equal to $5/3$).

Although this model introduced its own set of assumptions, it provided a great deal of new insight into the nature of the radio emission from CWBs. An immediate realization was the potential importance of the Razin effect in attenuating the low frequency synchrotron emission within the WCR. Several key scaling relationships were also established. For instance, the total synchrotron emission from the entire WCR in adiabatic systems was found to scale as $D^{-1/2}\nu^{-1/2}$, where D is the separation of the stars (for comparison, the X-ray emission in the optically thin, adiabatic limit, scales as D^{-1}). The importance of IC cooling was also highlighted, having been shown to be a significant effect even in wide systems. In fact, the neglect of IC cooling in this work resulted in an overestimate

of the high frequency synchrotron flux from WR 147.

Pittard et al. (2006) addressed the IC cooling of the downstream non-thermal electron distribution in a follow-up paper, and discovered that non-thermal electrons located near the contact discontinuity of the WCR suffered the greatest amount of IC cooling, leading to a dearth of emission from this region. Not surprisingly, the addition of IC cooling led to a significantly better fit between models and observations of WR 147. It also broke the previously identified relationship between the total synchrotron luminosity and the stellar separation noted by Dougherty et al. (2003). Instead, the *intrinsic* luminosity was now observed to *decline* with stellar separation as IC cooling became increasingly strong. The effect of the stellar separation on the *thermal* radio flux was also explored. It was discovered that the *thermal* radio emission from the WCR scales as D^{-1} , in an identical way to the thermal X-ray emission. Since this emission is optically thin in systems with an adiabatic WCR, it can mimic a synchrotron component, so that one should rather cautiously interpret data with a spectral index $-0.1 \lesssim \alpha \lesssim 0.5$ (Pittard et al. 2006).

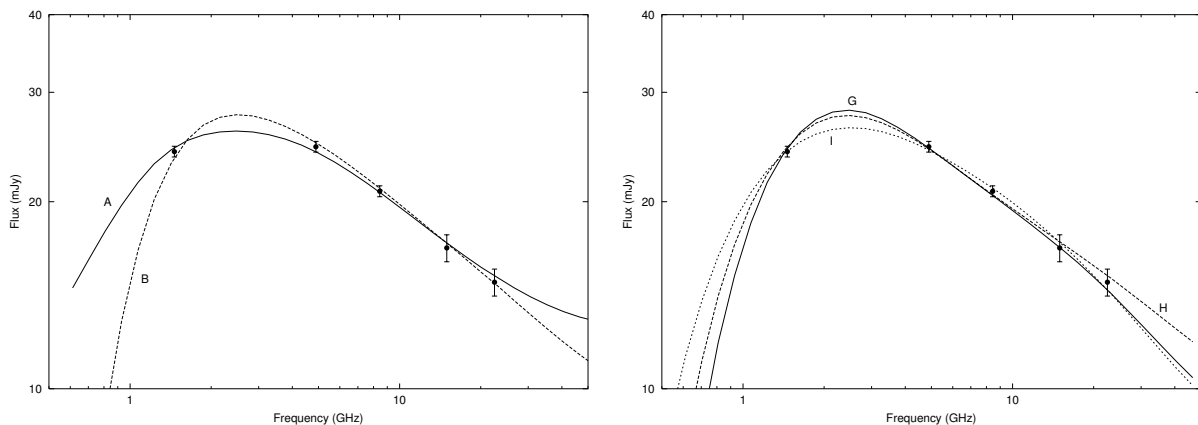


Figure 3: Model fits to the radio data of WR 140 at $\phi = 0.837$. Left: Fits where the low-frequency turndown is due to free-free absorption. Models A and B span plausible values of the wind momentum ratio, η . Right: Fits where the Razin effect is responsible for the turndown. For further details of the models see Pittard & Dougherty (2006).

The improved model was applied to WR 140 in Pittard & Dougherty (2006), with X-ray data further helping to constrain the mass-loss rates. Fits were obtained to data at orbital phase 0.837, which is around the peak of the non-thermal radio lightcurve and also when an ASCA dataset is available. It was discovered that the low frequency turndown in the radio spectrum could be explained as either free-free absorption through the surrounding stellar winds, or the Razin effect (see Fig. 3). In the former case it proved impossible to obtain a good fit to the data with $p = 2$. The best fit was obtained with $p = 1.4$, though changes to the assumed magnetic field strength allow this value to move slightly. Such indices can result from the shock re-acceleration process, whereby the non-thermal particles pass through a sequence of shocks (Pope & Melrose 1994), or from 2nd order Fermi acceleration. Either of these processes may be significant in CWBs, since the clumpy nature of the winds means that the WCR is likely to be highly turbulent, with weak shocks distributed throughout it (Pittard 2007). In contrast, fits with the Razin effect dominant do allow $p = 2$, though require a worryingly high efficiency of electron acceleration. For this reason, fits with free-free absorption dominant were preferred. A wide range of wind momenta could fit the data in this case, though it might be possible to constrain the models with future, high sensitivity VLBA observations. It might also be necessary to apply a rather extreme taper to better emphasize the lower spatial frequency content of the visibility data to tease out structure further downstream of the WCR apex where the opening angle of the WCR has reached its asymptotic limit.

2.2 Models of the Non-thermal X-ray and γ -ray Emission

In recent years there has been a revival of interest in non-thermal X-ray and γ -ray emission from CWBs, as the dramatic sensitivity gains achieved by space-based satellites and ground-based arrays of Cerenkov telescopes have raised the tantalizing prospect of the first detections. This, in turn, has led to new theoretical predictions. Amongst the first was a work by Bednarek (2005), who calculated the expected γ -ray emission from WR20a, a rare WR+WR binary. The short orbital period of this system means that the optical depth to electron-positron pair creation is high enough to initiate electromagnetic cascades. Due to this system's high optical depth to TeV photons, it cannot be directly responsible for nearby TeV emission (Aharonian et al. 2007), which more likely is the result of acceleration processes within the collective wind of the nearby cluster Westerlund 2.

A two-zone model for the non-thermal emission from CWBs was presented by Reimer et al. (2006). In their model, particles are accelerated in an inner zone where their spatial diffusion exceeds their motion due to advection with the background fluid. Relevant gain and loss mechanisms are considered in the computation of the energy distribution. Particles leave this region once the timescale for their diffusion exceeds their advection timescale. The particles are then assumed to move into an outer advection region where they suffer further losses as they flow downstream.

The anisotropic nature of the IC process is considered in the calculation of the expected flux, though the weaker of the two stellar radiation fields is ignored. Reimer et al. (2006) conclude that GLAST/Fermi should easily detect WR 140, though they expect that the large variation in the energy density of the stellar radiation fields resulting from the high orbital eccentricity is likely to obscure the effect of the change in the IC flux with viewing angle due to anisotropic scattering. However, Reimer & Reimer (2009) demonstrate that it is possible to constrain the orbital inclination of colliding wind systems through their nonisotropic IC emission.

A complementary model of the X-ray and γ -ray emission from WR 140 was presented by Pittard & Dougherty (2006). This work built on the phenomenological model developed previously by Dougherty et al. (2003) and Pittard et al. (2006) to explore the non-thermal radio emission. Here the energy spectrum is assumed rather than calculated, but the model benefits from a more realistic description of the density and temperature distribution within the system. Although Pittard & Dougherty (2006) adopt an isotropic treatment of the IC emission, they find that other uncertainties, such as the particle acceleration efficiency and the spectral index of their energy distribution (both of which remain ill-constrained from fits to radio data - see the previous section), have at least as much influence on the predicted flux as the angle-dependence of the IC emission. A key issue is that the degeneracy which exists between the models in the radio is broken at MeV-TeV energies, raising the possibility of future γ -ray detections allowing one to distinguish the nature of the low-frequency turnover, the acceleration efficiency of the non-thermal electrons, and the strength of the magnetic field. Several of the Razin fits have since been ruled out by the upper limits to the INTEGRAL emission obtained by De Becker et al. (2007).

Fits to the WR 140 radio data at other phases have been performed, and a good match to the radio lightcurve is now obtained (Pittard, in preparation). However, the fitted parameters change with orbital phase in a relatively complicated fashion which defies easy explanation.

2.3 Models of the Thermal Radio Emission

The effect of binarity on the thermal radio emission was investigated by Stevens (1995), who found that at a given orbital separation, the 2 cm radio flux increased as the wind momenta ratio became more uniform, and could exceed the single star value by up to 50%. More recently, Pittard (2010) showed that in short period O+O-star systems with a radiative WCR, the thermal emission from the WCR becomes optically thick, and can dominate the total radio flux from the system, exceeding

the combined flux from identically typed single stars by over an order of magnitude. This clearly would have a large impact on the derived stellar mass-loss rates in cases where the emission from the WCR is ignored. Radio lightcurves and spectra were also obtained. A strong hysteresis is seen in the synthetic lightcurve of a simulated eccentric system, reflecting the underlying hysteresis of the dynamics. Similar behaviour is seen in simulated X-ray observations (Pittard & Parkin 2010).

3 Future Research

3D models of the dynamics of the WCR have provided useful new insight into the nature of colliding wind systems. A full investigation of possible orbit and stellar parameters will undoubtedly occur over time. The continuing progress in computational power is making fully 3D simulations possible, though they are a long way from being routine.

In modelling non-thermal emission, a key area for progress will involve abandoning phenomenological models of the non-thermal emission in favour of a model in which the acceleration of the particles and their effect on the shock structure are self-consistently obtained. To develop such models will require the integration of an advection-diffusion equation for the non-thermal particles into the hydrodynamical codes. The advent of radio interferometers with increased sensitivity (e.g. the EVLA and e-MERLIN) will add significant numbers of newly detected radio CWBs, which will allow better comparison to the new models in progress.

Acknowledgements

I would like to express my sincere gratitude to the organizers for the invitation to present a review talk. I would also like to thank Sean Dougherty for many stimulating discussions, and the Royal Society for funding a University Research Fellowship which allowed the development of some of the research covered in this review.

References

- Aharonian, F., Akhperjanian, A. G., Bazer-Bachi, A. R., Beilicke, M., Benbow, W., Berge, D., Bernlöhr, K., Boisson, C., et al. 2007, *A&A*, 467, 1075
- Antokhin, I. I., Owocki, S. P. & Brown, J. C. 2004, *ApJ*, 611, 434
- Bednarek, W. 2005, *MNRAS*, 363, L46
- Chapman, J. M., Leitherer, C., Koribalski, B., Bouter, R. & Storey, M. 1999, *ApJ*, 518, 890
- De Becker, M., Rauw, G., Pittard, J. M., Antokhin, I.I., Stevens, I. R., Gosset, E. & Owocki, S. P. 2004, *A&A*, 416, 221
- De Becker, M., Rauw, G., Pittard, J. M., Sana, H., Stevens, I. R. & Romero, G. E. 2007, *A&A*, 472, 905
- Dougherty, S. M., Beasley, A. J., Claussen, M. J., Zauderer, B. A. & Bolingbroke, N. J. 2005, *ApJ*, 623, 447
- Dougherty, S. M., Pittard, J. M., Kasian, L., Coker, R. F., Williams, P. M. & Lloyd, H. M. 2003, *A&A*, 409, 217
- Dougherty, S. M., Williams, P. M. & Pollacco, D. L. 2000, *MNRAS*, 316, 143
- Fahed, R., Moffat, A. F. J., Zorec, J., et al. 2011, in *Proceedings of the 39th Liège Astrophysical Colloquium*, eds. G. Rauw, M. De Becker, Y. Nazé, J.-M. Vreux & P.M. Williams, *BSRSL* 80, 668
- Gayley, K. G., Owocki, S. P., Cranmer, S. R. 1997, *ApJ*, 475, 786
- Henley, D. B., Corcoran, M. F., Pittard, J. M., Stevens, I. R., Hamaguchi, K. & Gull, T. R. 2008, *ApJ*, 680, 705
- Henley, D. B., Stevens, I. R. & Pittard, J. M. 2003, *MNRAS*, 346, 773
- Henley, D. B., Stevens, I. R. & Pittard, J. M. 2005, *MNRAS*, 356, 1308
- Lemaster, M. N., Stone, J. M. & Gardiner, T. A. 2007, *ApJ*, 662, 582
- Lührs, S. 1997, *PASP*, 109, 504
- Luo, D., Mc Cray, R. & Mac Low, M.-M. 1990, *ApJ*, 362, 267
- Okazaki, A. T., Owocki, S. P., Russell, C. M. P. & Corcoran, M. F. 2008, *MNRAS*, 388, L39

- Parkin, E. R. & Pittard, J. M. 2008, MNRAS, 388, 1047
Parkin, E. R., Pittard, J. M., Corcoran, M. F., Hamaguchi, K. & Stevens, I. R. 2009, MNRAS, 394, 1758
Pittard, J. M. 2007, ApJ, 660, L141
Pittard, J. M. 2009, MNRAS, 396, 1743
Pittard, J. M. 2010, MNRAS, 403, 1633
Pittard, J. M., Corcoran, M. F. 2002, A&A, 383, 636
Pittard, J. M., Dobson, M. S., Durisen, R. H., Dyson, J. E., Hartquist, T. W. & O'Brien, J. T. 2005b, A&A, 438, 11
Pittard, J. M. & Dougherty, S. M. 2006, MNRAS, 372, 801
Pittard, J. M., Dougherty, S. M., Coker, R. F. & Corcoran, M. F. 2005a, in "X-Ray and Radio Connections", eds. L.O. Sjouwerman and K. K Dyer, published electronically by NRAO, <http://www.aoc.nrao.edu/events/xraydio>
Pittard, J. M., Dougherty, S. M., Coker, R. F., O'Connor, E. & Bolingbroke, N. J. 2006, A&A, 446, 1001
Pittard, J. M. & Parkin, E. R. 2010, MNRAS, 403, 1657
Pittard, J. M. & Stevens, I. R. 2002a, A&A, 388, L20
Pollock, A. M. T., Corcoran, M. F., Stevens, I. R. & Williams, P. M. 2005, ApJ, 629, 482
Pope, M. H. & Melrose, D. B. 1994, PASA, 11, 175
Reimer, A., Pohl, M., Reimer, O. 2006, ApJ, 644, 1118
Reimer, A. & Reimer, O. 2009, ApJ, 694, 1139
Stevens, I. R. 1995, MNRAS, 277, 163
Stevens, I. R., Blondin, J. M. & Pollock, A. M. T. 1992, ApJ, 386, 265
Stevens, I. R. & Pollock, A. M. T. 1994, MNRAS, 269, 226
Stevens, I. R., Corcoran, M. F., Willis, A. J., Skinner, S. L., Pollock, A. M. T., Nagase, F. & Koyama, K. 1996, MNRAS, 283, 589
Strickland, R. & Blondin, J. M. 1995, ApJ, 449, 727
Vishniac, E. T. 1983, ApJ, 274, 152
Vishniac, E. T. 1994, ApJ, 428, 186
Walder, R. 1998, Ap&SS, 260, 243
White, R. L. & Becker, R. H. 1995, ApJ, 451, 352
Williams, P. M., Dougherty, S. M., Davis, R. J., van der Hucht, K. A., Bode, M. F. & Setia Gunawan, D. Y. A. 1997, MNRAS, 289, 10
Williams, P. M., van der Hucht, K. A., Pollock, A. M. T., Florkowski, D. R., van der Woerd, H. & Wamsteker, W. M. 1990, MNRAS, 243, 662

Discussion

P. Williams: Many of the colliding wind systems with carbon-rich Wolf Rayet stars have dust. Chemical models for dust formation require overdensities of many orders of magnitude. Are you seeing these in your models?

J. Pittard: Yes, if there is strong cooling, it is in principle very easy to obtain large overdensities. One may first obtain a factor of 4 increase in density at the shock, and then as gas cools from $\sim 10^4\text{K}$ to $\sim 10^3\text{K}$ one can get up to another factor of $\sim 10^4$ increase in overdensity. Having said this, as the gas cools and is compressed, the magnetic field may start to exert a significant pressure and thereby moderate the overall increase in density to some extent.

J. Groh: Related to Prof. Williams' question, what's the minimum temperature you achieve in the overdense regions of your simulations?

J. Pittard: All our simulations have a floor temperature of 10^4K , which is also assumed to be the wind temperature. However, in reality the temperature will be set by the balance between photoionization heating and radiative cooling. We do not include photoionization in our current models. In principle, we should be able to reach temperatures $\sim 10^3\text{K}$ as indeed is observed when dust forms.